ACS OMEGA

Open Access

http://pubs.acs.org/journal/acsodf

Article

Unconventional Reservoir Characterization of Patala Formation, Upper Indus Basin, Pakistan

Muhsan Ehsan,* Rujun Chen,* Muhammad Ali Umair Latif, Kamal Abdelrahman, Abid Ali, Jar Ullah, and Mohammed S. Fnais

Cite This: *ACS Omega* 2024, 9, 15573−15589

Read Online

ACCESS | Metrics & More | Article Recommendations

ABSTRACT: Unconventional hydrocarbon exploration is needed in the current oil and gas crisis scenario. Therefore, the development of conditions for unconventional hydrocarbon exploration is needed. In the Upper Indus Basin (UIB), Pakistan, the Patala Formation is one of the potential candidates for this unconventional exploration. It is a proven source rock at the regional level in the Kohat-Potwar sub-basin of UIB. This study aims to evaluate the shale gas potential of the rock in the Minwal-Joyamair area of the sub-basin. Developing a shale rock physics model is important for exploring and developing shale reservoirs due to the difference between unconventional shale and conventional sand reservoirs. These differences include mineral types, mineral characteristics, matrix pores, and fluid properties. To achieve the study's objectives, an integrated strategy provides for evaluating rock physics parameters, petrophysics, and geochemical analyses. This integrated approach indicates that the Patala Formation is a good potential reservoir for shale gas exploration. The Formation has a significant thickness (around 40−50 m), higher total organic carbon content (02−10%), higher brittleness index (0.44−0.56), and relatively shallow depth (2136−3223 m). These research findings suggested that the presence of organic and quartz-rich lithofacies can be considered as highly favorable "sweet spots" for shale-gas exploration in the UIB, Pakistan. Through proper understanding of the spatial and temporal distribution of these "sweet spots", shale-gas exploration can be developed as an effective strategy to exploit shale gas.

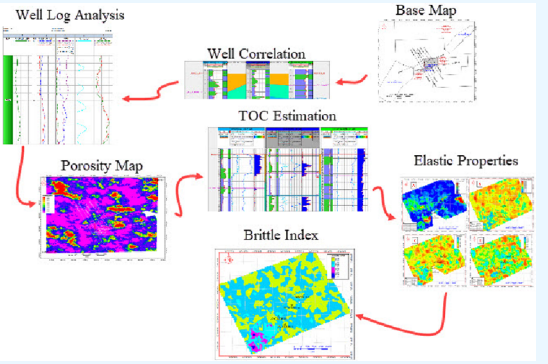

1. INTRODUCTION

Shale gas exploration and research are becoming increasingly popular due to the global energy shift, depletion of conventional hydrocarbon resources, and their long-term potential and financial sustainability.[1] One crucial element influencing the distribution of oil and gas resources is the spatiotemporal distribution of source rocks.[2] The Patala Formation in this basin is a proven principal source rock and is considered a potential unconventional resource. Past studies do not provide comprehensive information regarding the presence of unconventional resource potential of the sub-basin. The lithologic attributes, total organic carbon (TOC) content, and greater stratigraphic thickness of the Formation make it a potential candidate for shale gas in the sub-basin. Fewer wells are drilled up to the level of the Patala Formation. Therefore, an in-depth study is required to evaluate the suitability of this formation for the shale gas potential.[3,4]

Hydraulic fracturing has been extensively utilized in global oil and gas exploration and production. It has developed into a vital method in the past 10 years for increasing the output of hydrocarbons from unconventional reservoirs. In this study, we learn more about how bedding characteristics affect shale's mechanical properties, such as permeability, compressive strength, and tensile strength.[5] The lower primary porosity and extremely low permeability of organic-rich shale, the abundance of clay minerals (platy), the density of the minerals, the variability in the brittle and ductile zones, and preservation conditions are the critical factors of a potential shale gas resource.[6−8] These petrophysical and geomechanical parameters are important for unconventional hydrocarbon exploration and development, requiring a detailed analysis of shale-gas reservoirs.[9−12] A complete suite of well logs is essential for understanding the detailed petrophysical characteristics such as TOC estimation, kerogen type, porosity, density, velocity, and resistivity of shales. The mineral classifications of the given shales are also an essential factor for this purpose.[13−15]

Received: January 15, 2024
Revised: March 3, 2024
Accepted: March 7, 2024
Published: March 21, 2024

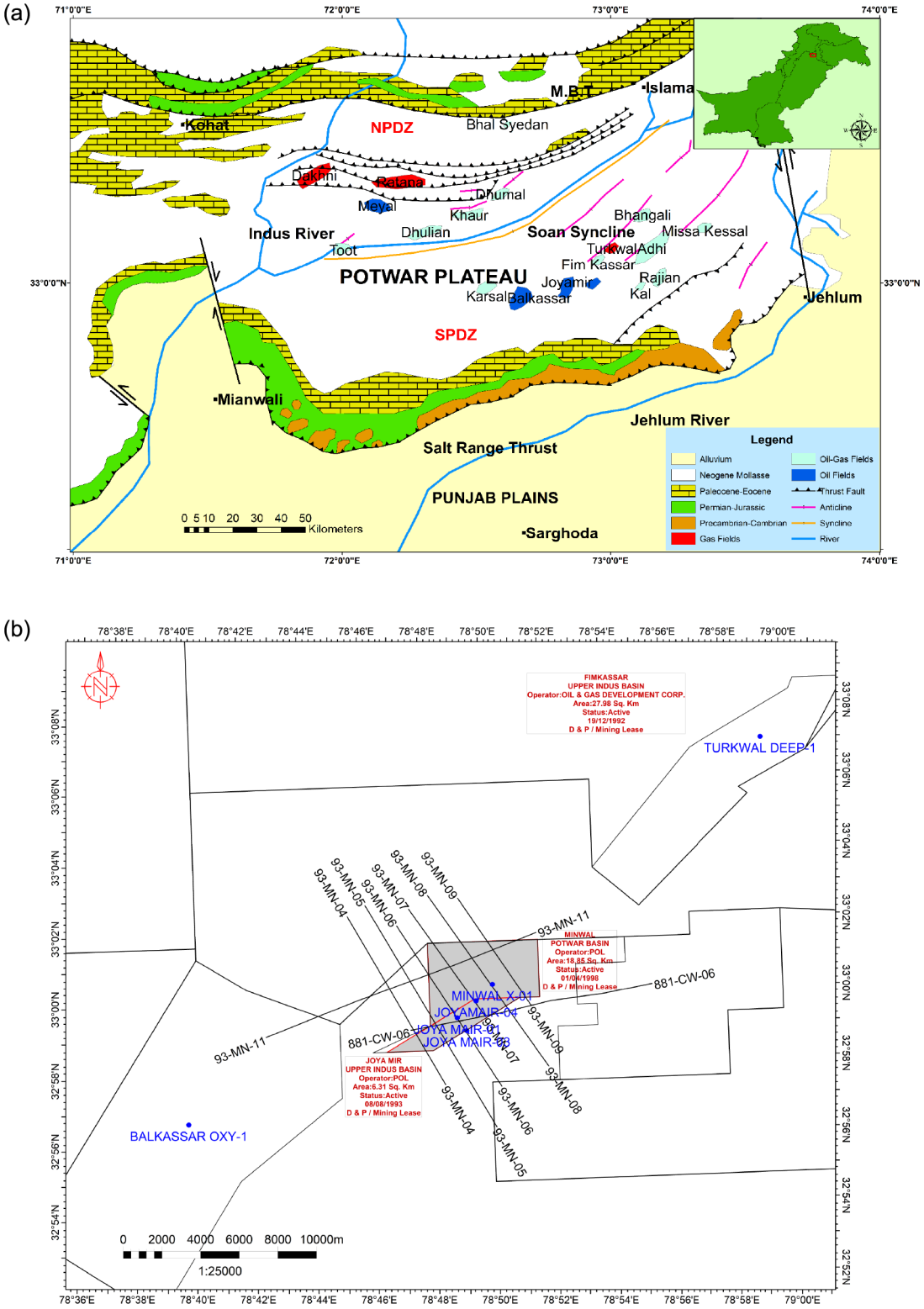

Figure 1. (a) Geological map with index map of Pakistan showing the position of Minwal-Joyamair with adjoining fields (modified and updated from refs24 and25. (b) Base map of the study area with 2D seismic profiles and wells.

In recent years, the oil and gas industry has experienced a significant surge in interest in extracting unconventional hydrocarbons from shale source rocks. This increased interest can be attributed to the depletion of conventional resources and the state-of-the-art technologies in directional drilling and hydraulic fracturing techniques.[16,17] Assessing unconventional shale-gas reservoirs poses several exploration challenges, primarily due to their heterogeneous lithology, which reflects long-term changes in depositional environments and spatially varying diagenetic influences that alter the permeability values, which makes it more complex to explore them.[9] Unconventional (shale-gas) reservoirs require advanced technologies

https://doi.org/10.1021/acsomega.4c00465
ACS Omega 2024, 9, 15573−15589

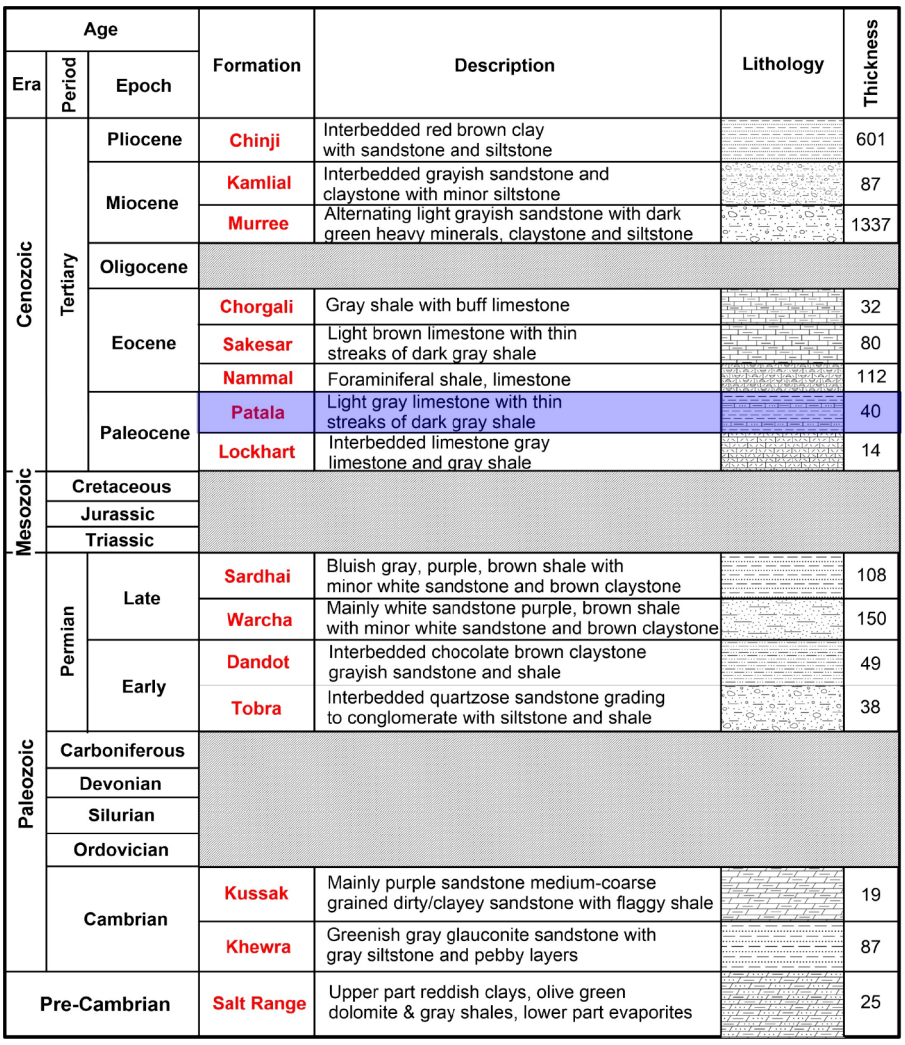

Figure 2. Borehole stratigraphic column for the Joyamair Oil Field, Kohat-Potwar Plateau, Pakistan.

such as multistage hydraulic fracturing to attain maximum hydrocarbon production, as the shales have less effective permeability.[18] This operation of multistage hydraulic fracturing creates a fracture network swamp that depends on the brittle and ductile behavior of the shale. Several studies have characterized shale gas reservoirs using petrophysical and geochemical approaches.[6,19]

Shale gas reservoirs have been examined extensively over the years. Still, little is known about the origin and development of their pore systems, which is a crucial parameter from an exploration point of view. Characterizing shale characteristics, whose sizes range from nm to μm, is challenging.[20] The shale-gas potential of organic-rich shale is affected by its permeability (a function of its porosity and pore structure). The permeability affects gas flow rates and mechanical properties (e.g., elastic properties, which affect in situ stresses and brittleness). These impact the hydraulic fracturing operations typically required to achieve the economic production rates. Different types of porosity systems exist within organic-rich shales (e.g., kerogen pores, interparticle, intraparticle, and fracture-type pores). Permeability provides a direct estimate of shale gas potential and can be used to determine the productivity of shale gas reservoirs.[21−23]

In this study, integrated research was established by utilizing the fundamental petrophysical and geomechanical rock properties studies to determine the detailed potential of Patala, focusing mainly on Minwal and Joyamair areas (Figure 1a,b). Empirical equations utilizing well logs, such as density, sonic, and resistivity, have demonstrated rapid predictions and achieved reasonably accurate results through the ΔlogR method. However, seismic data sets have not been thoroughly investigated as potential inputs for reliable predictions of TOC in the study area. Additionally, while several studies have estimated TOC using well-logging data for different formations, there is limited research conducted on predicting TOC for the Patala Formation. In this study, the source rock potential of the Patala Formation was evaluated using conventional well logs. The shale-gas reservoir attributes such as TOC, porosity, thickness, and depth were determined. Additionally, rock physics and geomechanical parameters such as brittleness cross-plots were yielded to distinguish the Formation's brittle, ductile, and transitional zones.

2. GEOLOGICAL SETTINGS AND STRATIGRAPHY

Potwar sub-basin is a part of the Upper Indus Basin (UIB) in which the Precambrian Indian Shield (basal crystalline rocks) is covered by a substantial sedimentary succession of Phanerozoic to recent rocks.[1,26,27] The UIB is further subdivided into Potwar (East) and Kohat (West) sub-basins, which the Indus River separates. Both sub-basins are

https://doi.org/10.1021/acsomega.4c00465
ACS Omega 2024, 9, 15573−15589

Table 1. Patala Formation Thickness in the Surrounding Wells

well name	surface	formation top (MD)	thickness (m)
Balkassar Oxy-01	Patala	2602.87	21.33
Chak Naurang-01	Patala	2312.50	13.70
Joyamair-03	Patala	2212.80	40.00
Joyamair-04	Patala	2136.65	39.62
Turkwal Deep-01	Patala	3223.56	26.83
Khaur Oxy-01	Patala	1869.86	68.57

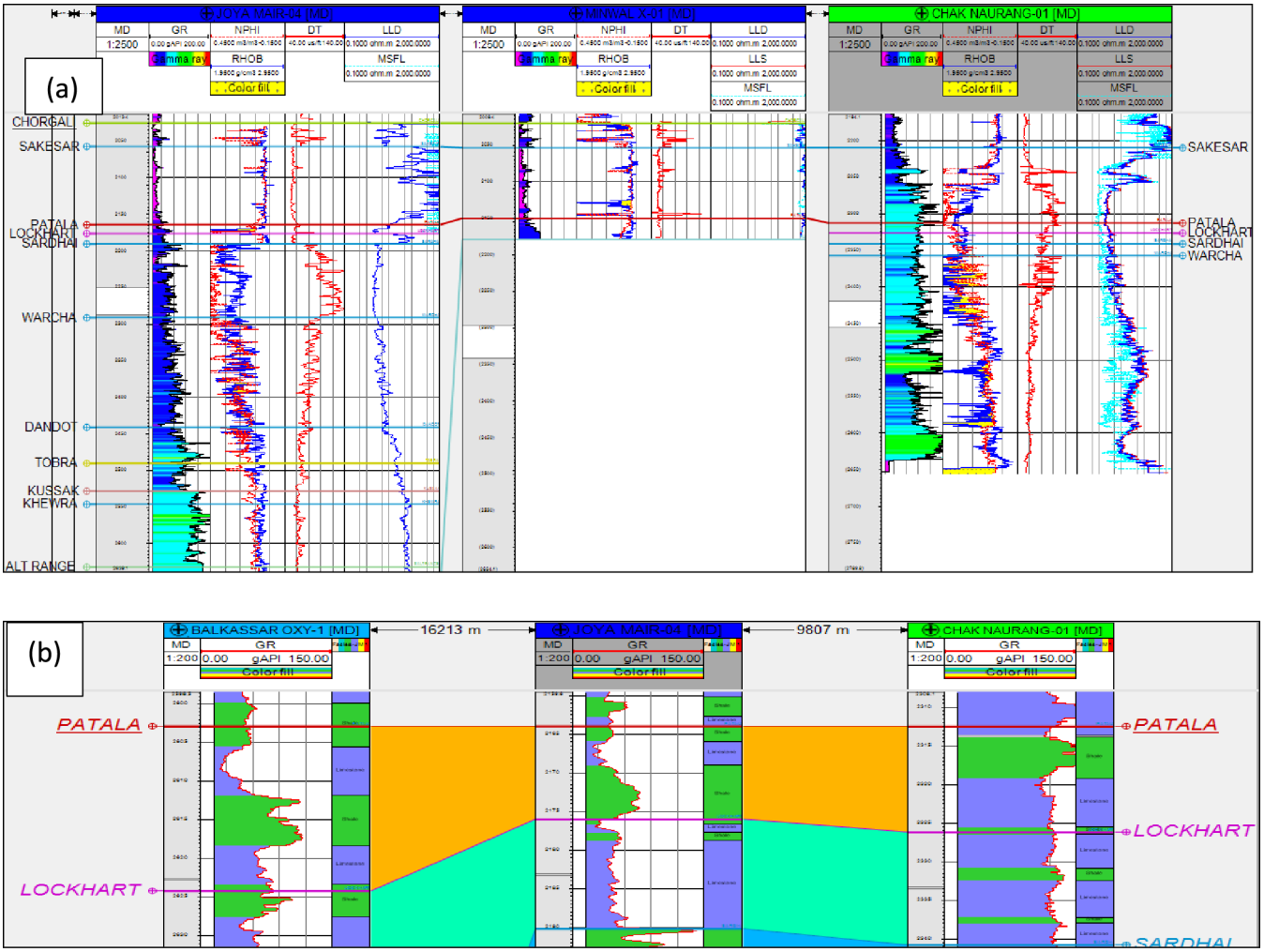

Figure 3. (a) Stratigraphically well correlation of available well log data facilitating comprehensive well logs interpretation. This correlation provides invaluable insights into the distribution of subsurface petrophysical properties. (b) Well correlation for Patala Formation thickness is a crucial component of subsurface analysis in this study. This correlation enables the identification of regional trends and variations in the thickness within the target formation.

tectonically deformed and represent facies variations (Figure 1). Potwar sub-basin was formed as a result of a head-on collision between Eurasian and Indian plates during the Eocene, and it depicts the active deformation of the Himalayan foreland in Pakistan.[28] It is bounded by Main Boundary Thrust (MBT), Salt Range Thrust (SRT), and Jehlum and Kalabagh strike-slip faults in the north, south, east, and west directions, respectively.[29] It is considered to be one of the most prolific oil provinces in northern Pakistan.

The Cambrian to Eocene platform sequence is deposited over the Salt Range Formation in the study area, as shown in Figure 2. The Salt Range Formation (Eocambrian) is overlaid by the Early to Middle Cambrian Jehlum Group in the study area. The Cambrian Khewra and Kussak Formations are part of the Jehlum Group. These units were deposited in marine to shallow marine sedimentary environments. No sediment was deposited in the Salt Range Potwar Foreland Basin because the basin was raised during the Ordovician to Carboniferous period. The Permian Nilawahan Group disconformably overlies the Jehlum Group, which comprised Tobra, Dandot, Warcha, and Sardahi Formations. In the sub-basin, the Late Permian Zaluch Group was either not deposited or eroded due to uplift (Pre-Paleocene). The Paleocene to Eocene carbonate-shale series was thickly deposited due to early Paleocene marine transgression. The Lockhart, Patala, Sakesar, and Chorgali formations are part of it. The primary reservoirs for

https://doi.org/10.1021/acsomega.4c00465
ACS Omega 2024, 9, 15573−15589

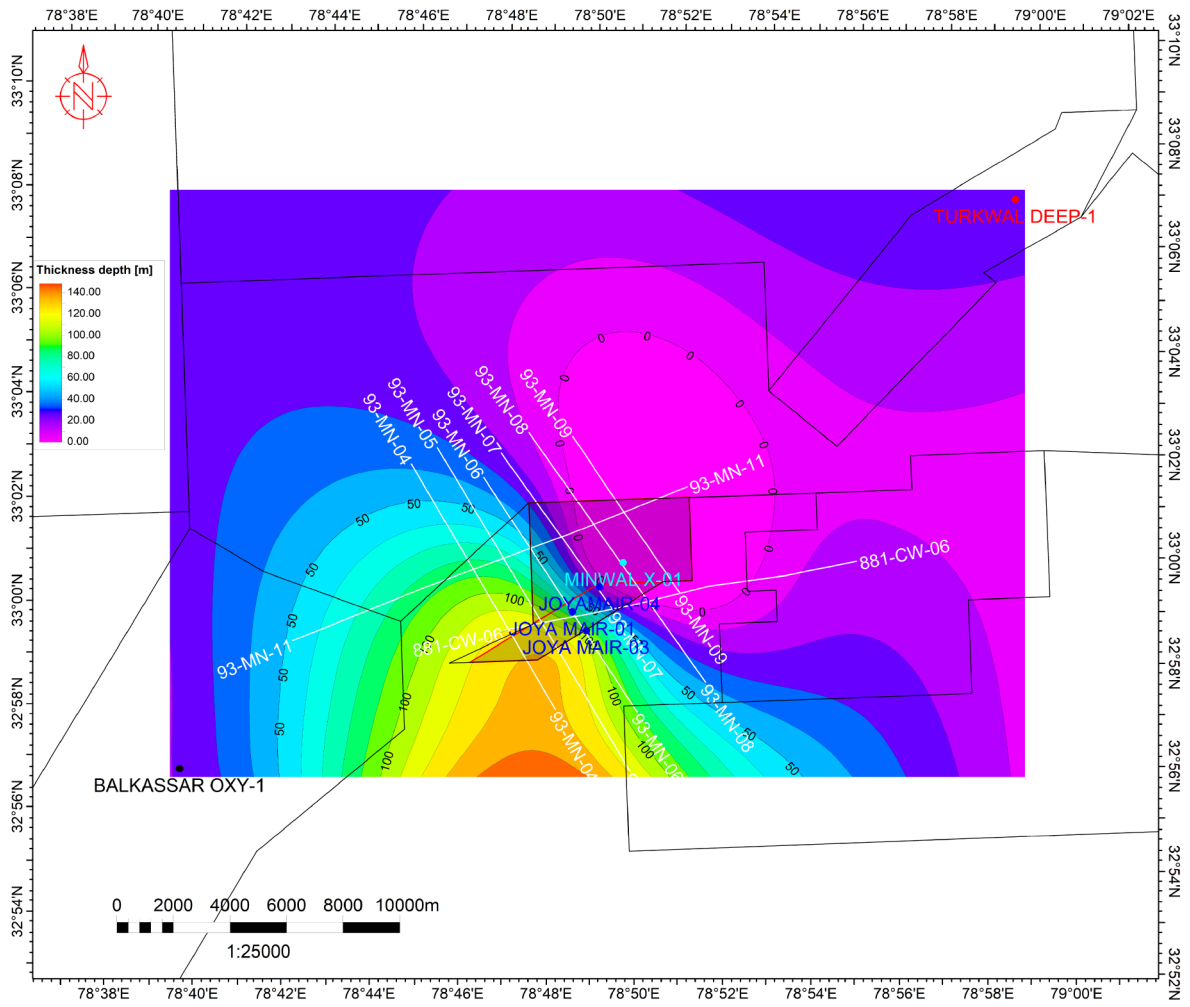

Figure 4. Patala Formation thickness map.

oil buildup in the region are the carbonates of these formations.[1,29]

Potwar Basin includes some significant formations from a hydrocarbon perspective, such as the Late Paleocene Patala Formation. The Patala Formation's carbonaceous shales and coal beds serve as a possible source rock for numerous tertiary reservoirs in the Kohat Basin. These resources enhance the Patala Formation's hydrocarbon source rock assessment in the Potwar Basin. The formation is well developed and exposed in the Salt Range, Kala-Chitta Range, Kohat, and Hazara localities.[30−32] The Early Paleocene Hangu, Middle Paleocene Lockhart, and Late Paleocene Patala formations are among the shallow marine depositional units.[33] The Patala Formation predominantly comprises gray to greenish-gray color splintery shale units. Shales are organically rich and bear glauconite.[34] The Patala Formation exhibits a stratigraphy characterized by thin layers of marl and gypsum intercalations alongside medium- to thick-bedded carbonaceous (rich in organic content) shale. The shale is notably fossil-rich and occasionally displays laminations.[35]

3. MATERIALS AND METHODS

Borehole logs data from Balkassar OXY-01, Joyamair-04, and Chaknaurang-01 wells were utilized to estimate TOC, porosity, mineral content, kerogen volume, and rock elastic properties of the Patala Formation. Well-top information was used to develop a thickness map. Additionally, 2D seismic lines were interpreted for structural analysis, focusing mainly on the hydrocarbon accumulation and preservation of the shale gas (Figure 1b). Table 1 describes the well data used for Patala Formation thickness mapping. The gamma ray (GR) log curve and other composite logs were utilized to create a cross section along the regional line, which extends from the east (Balkassar) to the west (Chaknaurang) (Figure 3a). According to structural analysis, the Patala Formation exhibits a considerable thickness increase from the east to the west of the study area (Figure 3b).

3.1. Estimation of the TOC from Well Logs. The density (Schmoker's) method calculates TOC values using a linear relationship between bulk density and TOC. The Passey ΔlogR method estimates TOC by incorporating porosity and resistivity.[36] This study used the Schmoker and Passey methods for better correlation and estimation.

3.1.1. Schmoker's Method. Generally, a shale matrix has an average density of 2.7 g/cm^3. In comparison, the density of the organic matter ranges from 1.1 to 1.39 g/cm^3, which means that density log values are affected by organic contents. This method categorized shale content into four categories: rock matrix, pyrite, inter pores, and organic matter.[37] The following expression (eq 1) can give bulk density:

https://doi.org/10.1021/acsomega.4c00465
ACS Omega 2024, 9, 15573−15589

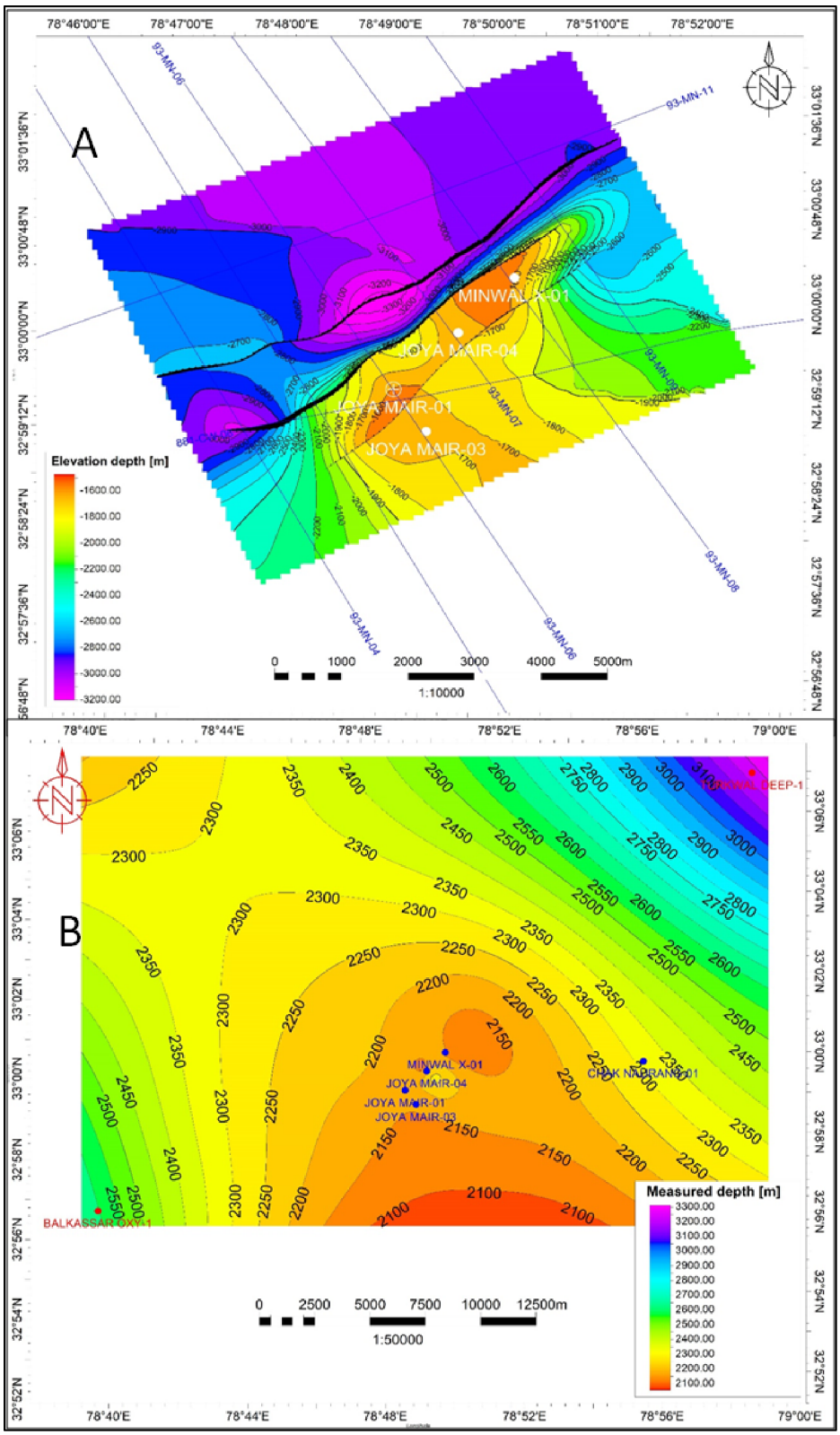

Figure 5. (A) Patala Formation depth (subsea) structure map using seismic interpretation. (B) Patala Formation depth (subsea) structure map using well tops.

$$\mathrm{TOC(wt.\ \%)} = \frac{154.497}{\rho_b} - 57.261 \quad (1)$$

where ρ_b is bulk density.

3.1.2. Passey ΔlogR Method. The ΔlogR method[38] is considered more appropriate in the petroleum industry. This Passey's method requires multiple well-log data to calculate the organic content of a formation. This method uses sonic, neutron, and density logs (eq 2) with resistivity logs and

https://doi.org/10.1021/acsomega.4c00465
ACS Omega 2024, 9, 15573−15589

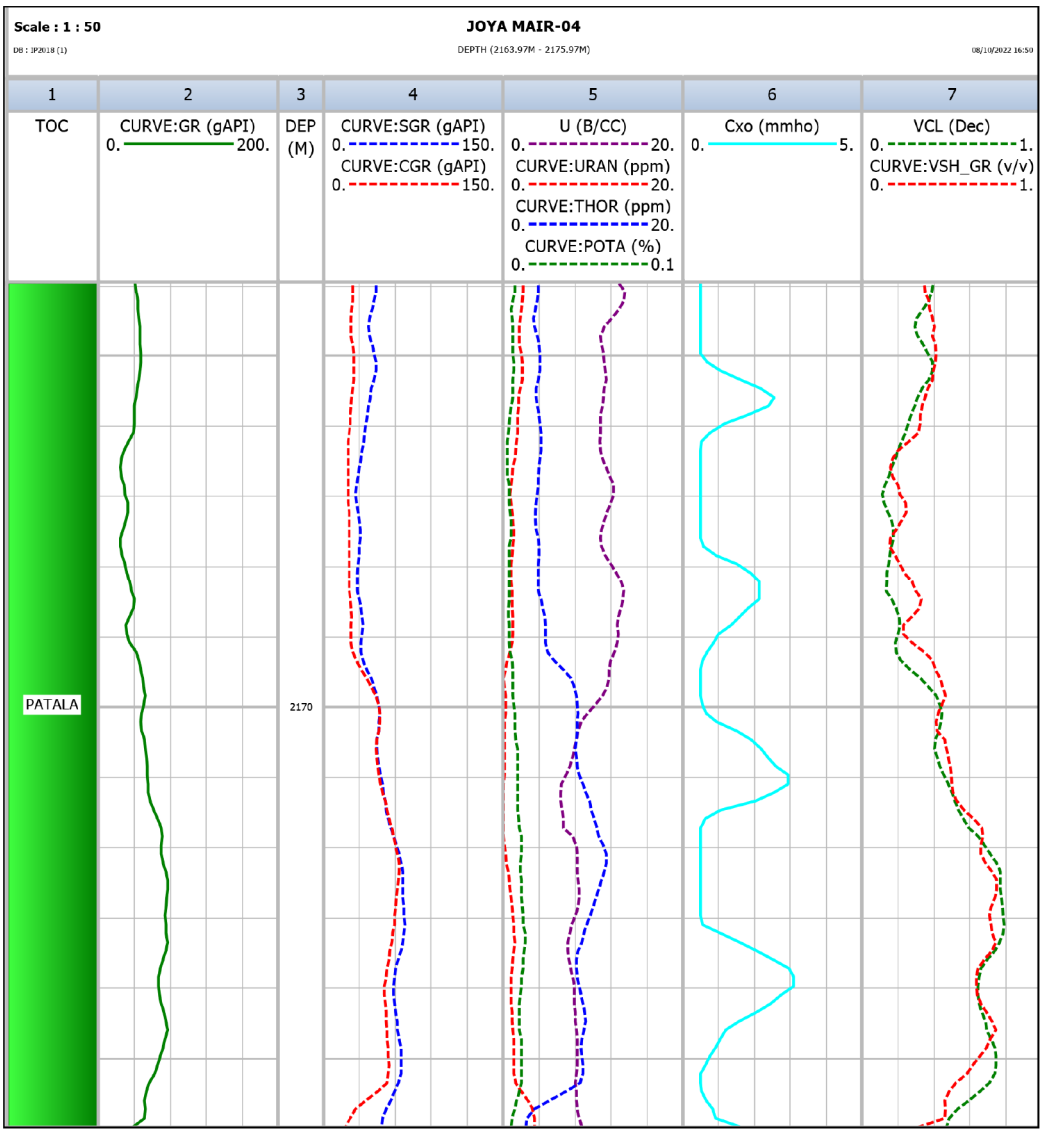

Figure 6. Spectral gamma ray log (SGR) correlation for mineral classification for the Patala Formation.

coefficients to calculate TOC. Then, ΔlogR can be estimated with the appropriate trendline to establish a relationship between TOC and ΔlogR.

The following are commonly used equations to estimate TOC by the ΔlogR method:

$$\Delta\log R_{\text{sonic}} = \log_{10}\left(\frac{R}{R_{\text{baseline}}}\right) + 0.02^{*}(\Delta t - \Delta t_{\text{baseline}}) \tag{2}$$

$$\Delta\log R_{\text{Neutron}} = \log_{10}\left(\frac{R}{R_{\text{baseline}}}\right) + 4.0^{*}(\Phi_N - \Phi_{N-\text{baseline}}) \tag{3}$$

$$\Delta\log R_{\text{Density}} = \log_{10}\left(\frac{R}{R_{\text{baseline}}}\right) + 2.5^{*}(\rho_{\text{b}} - \rho_{\text{b-baseline}}) \tag{4}$$

where R is resistivity, R_{baseline} is resistivity when resistivity and sonic curves baseline in a nonsource shale (ohm-m), Δt is sonic transit time (μs/meter), $\Delta t_{\text{baseline}}$ is travel time when resistivity and sonic curves baseline in a nonsource shale (μs/meter), Φ_N is neutron porosity, $\Phi_{N-\text{baseline}}$ is neutron porosity when resistivity and neutron curves baseline in a nonsource shale, and $\rho_{\text{b-baseline}}$ is bulk density when resistivity and density curves baseline in a nonsource shale (g/cm^3).[38]

In the present study, the following equations were used to determine ΔlogR and TOC using sonic and resistivity logs, respectively:

$$\text{TOC} = \Delta\log \text{R} \times 10^{(2.297-0.168\text{LOM})} + \Delta\text{TOC} \tag{5}$$

where LOM is amount of level organic metamorphism and ΔTOC is regional background level.[38]

Schmoker and Hester (1983)[39] correlated both TOC and density log. The usefulness of the density log can be limited due to its sensitivity to the conditions within the borehole and the presence of heavy metals like pyrite, which challenges its applicability.[38] TOCs are calculated by using the regression method of density and ΔlogR. TOC_final is the average output of all of the computed log curves used in different iterations. S_2 was calculated from ΔlogR. A cross-plot between S_2 and TOC gives the kerogen type and its maturity.

https://doi.org/10.1021/acsomega.4c00465
ACS Omega 2024, 9, 15573−15589

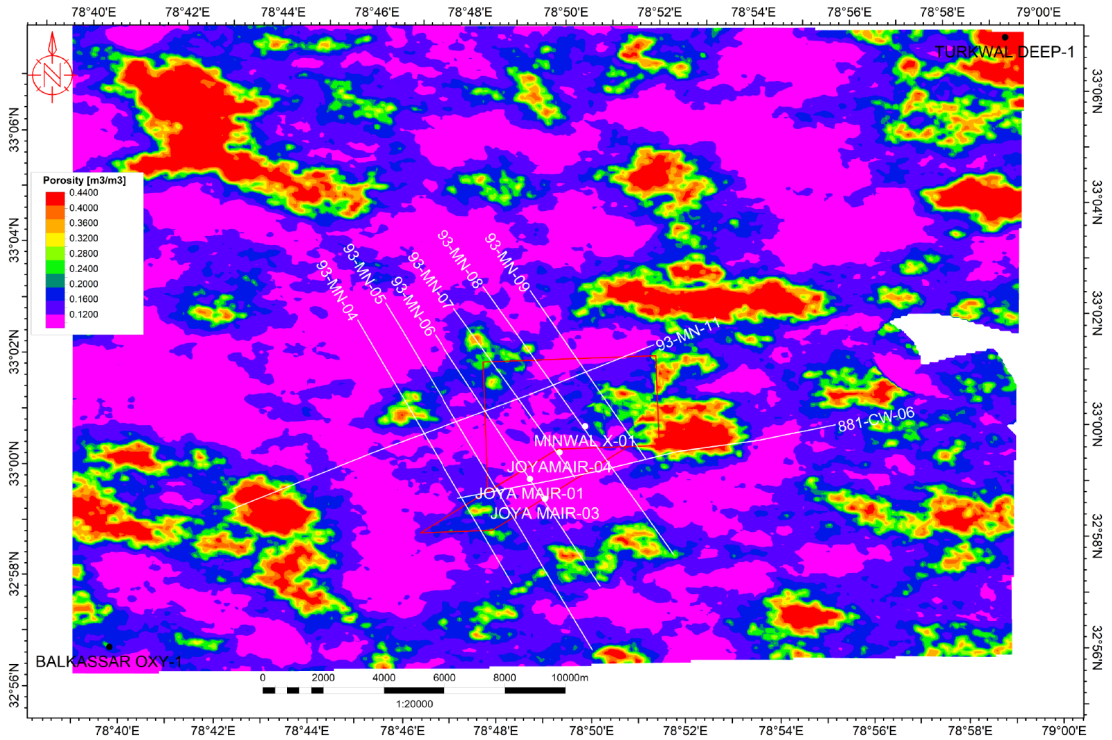

Figure 7. Porosity distribution map of the Patala Formation.

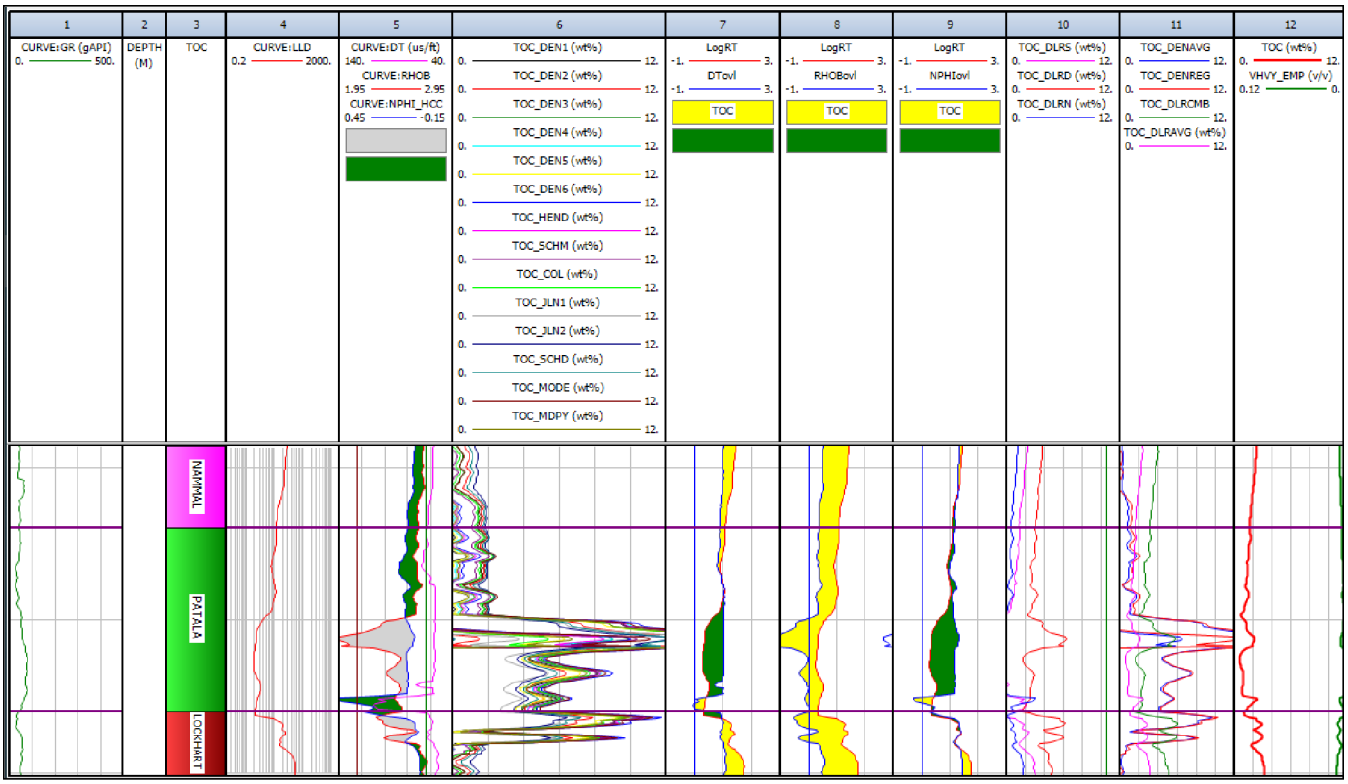

Figure 8. TOC calculations performed by using different methodologies and different well logs.

Previous studies have reported that the conventional well log data sensitive to organic content primarily include natural gamma ray, resistivity, transit interval time, density, and neutron logging. Higher organic matter content may generally lead to more pronounced deviations in these logs. Applying this principle makes it possible to identify source rocks and estimate the TOC and the S_1 and S_2 content. Since individual log parameters can be influenced by factors such as mineral composition, water, and pressure, it is necessary to utilize multiple log parameters to predict the TOC content accurately.[40]

https://doi.org/10.1021/acsomega.4c00465
ACS Omega 2024, 9, 15573−15589

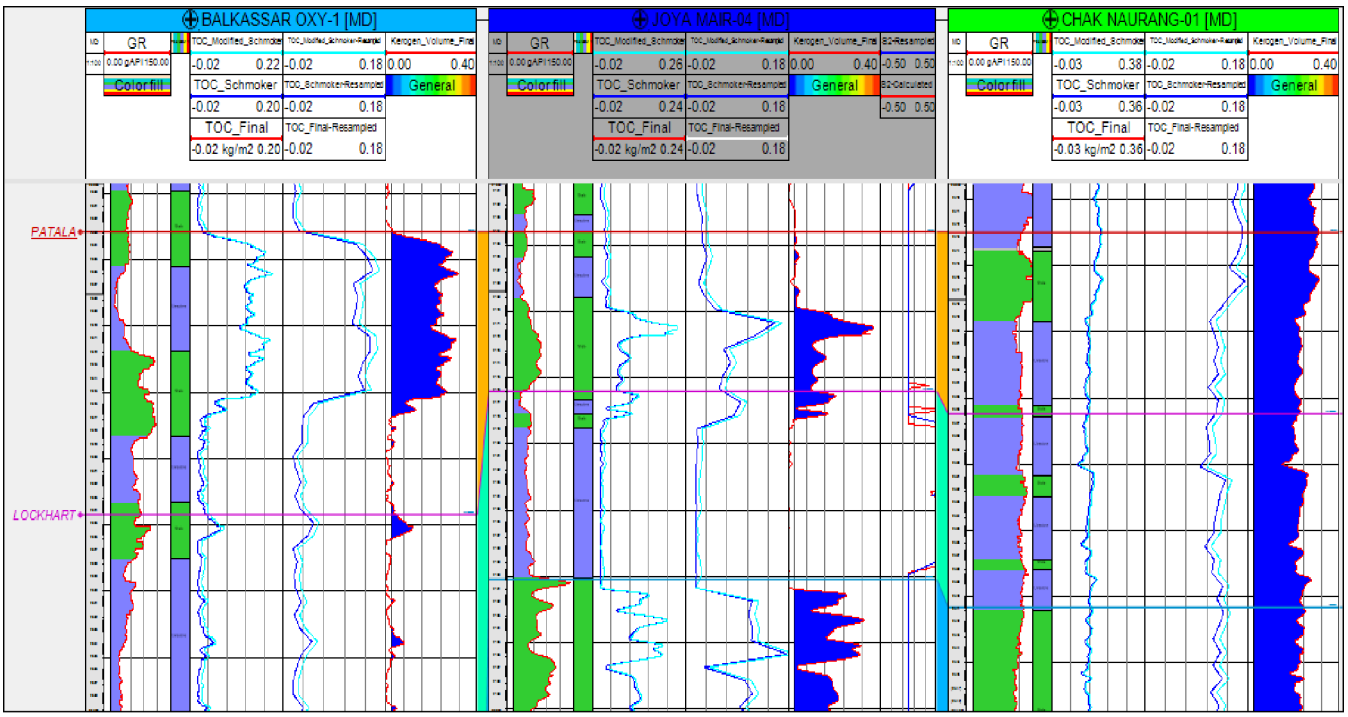

Figure 9. Regional well correlation for the TOC estimation.

3.2. Elastic Properties. Rock physics was computed from the given well logs, which output different types of moduli, which can help determine the physical and petrophysical properties of a given formation (Patala Formation). The result rock physics log curves are then populated in the static model, generating the distributing maps. The Lambda-Rho attribute is a fluid indicator, and as demonstrated in the well-based cross-plot analysis, a low value indicates the presence of sand, while a much lower value indicates the presence of hydrocarbon-bearing sand, while a high-value response corresponds to shale lithology. In most of the research related to the shale gas play exploration, rock elastic parameters such as Young's modulus (eq 6) and Poisson's ratio (eq 7)[41] in addition to mineralogical variation in a rock are used to define brittleness index (BI).

$$E = \frac{\rho_b \times V_s^2(3V_p^2 - 4V_s^2)}{(V_p^2 - V_s^2)} \quad (6)$$

$$\nu = \frac{V_p^2 - 2V_s^2}{2(V_p^2 - 2V_s^2)} \quad (7)$$

where E is Young's modulus, υ is dynamic Poisson's ratio, ρ_b is bulk density, and V_p and V_s are compressional and shear wave velocities, respectively.

Some researchers referred to it as a helpful correlation between the quartz content and fracture density. A higher content of clay minerals and an increased abundance of organic matter result in decreased BI.[42]

4. RESULTS AND DISCUSSION

4.1. Thickness and Depth of the Formation. It is widely recognized that shale, which is extensively distributed, serves as a good candidate for shale gas generation. A specific thickness of shale is a prerequisite for the enrichment of shale gas. Additionally, shale thickness plays a significant role in determining the abundance of shale gas resources. The deposition thickness serves as a prerequisite, ensuring the presence of organic matter and the reservoir space. The commercial accumulation of shale gas necessitates an adequate thickness and specific burial depth of shale.[43] The thickness of the Patala Formation varies from 12 to 95 m in the Minwal-Joyamair Field.[44] Therefore, the Minwal-Joyamair Field is suitable for shale-gas exploration with moderate depth and clean shale content within the Formation. Although the thickness of the Patala Formation is more significant compared to the neighboring fields (i.e., Balkassar and Chaknaurang) (Figure 4), the depth of the Formation is less as compared to those of these fields, which makes the study feasible for shale-gas potential assessment (Figure 5a). Patala Formation top and its thickness corresponding to wells show a considerable change in the Patala Formation thickness from Balkassar to Turkwal Field (Figure 1a,b). The depth of the Formation determined from the well top information and the one from the seismic data were quite comparable. The depth of the Patala Formation is not much more profound, which is also a positive aspect of unconventional exploration (Figure 5b).

4.2. Petrophysical Analysis. Petrophysical characterization of the unconventional shale-gas reservoir is still challenging due to their lithological and facies heterogeneity and anisotropic properties.[45] Petrophysical interpretation was performed on available well-log data. The unconventional reservoir has low effective porosity and microscale permeability, which must be considered. Available well-log data were utilized in the present study to conduct petrophysical analysis. Despite the data limitations, the petrophysical model was to derive the empirical relationships to estimate the TOC using the well log information on available well sites.

4.2.1. Shale Volume Estimation. The volume of shale can be estimated through well-logging data. The best logs for estimating the volume of shale are the gamma-ray log and its spectral components.[46] Uranium (U) content can help to

https://doi.org/10.1021/acsomega.4c00465
ACS Omega 2024, 9, 15573−15589

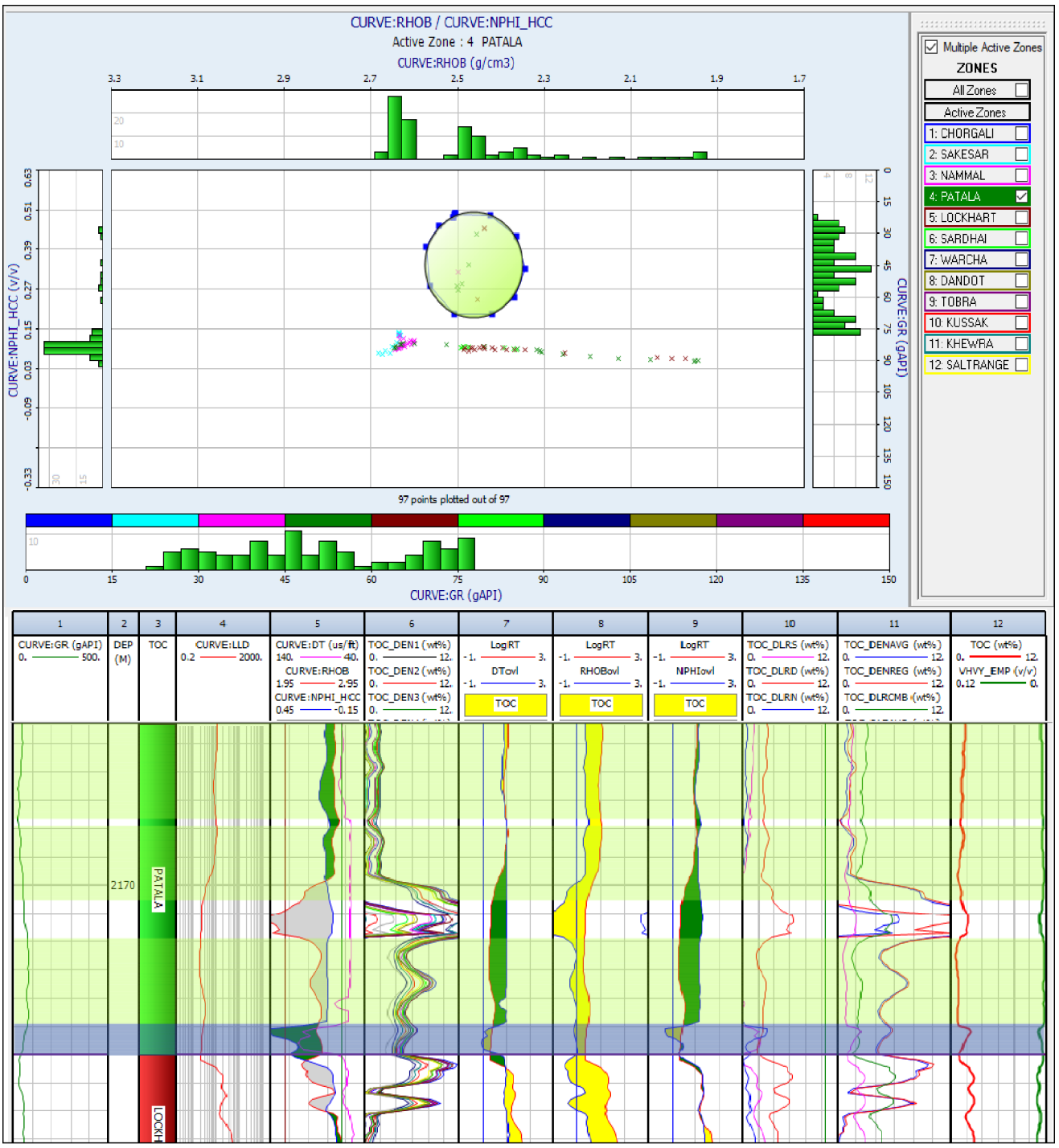

Figure 10. Neutron porosity (NPHI) vs density (RHOB) log cross-plot for TOC porosity estimation.

assess the organic matter abundance, and the TOC increases with the decrease of the uranium−thorium ratio. Therefore, using the regression analysis method, a natural gamma ray log can give TOC values.[47] The first step to calculate the volume of shale (Vsh) is to analyze and calibrate the GR in light of prospective shale units. The estimate of shale volume in the respective formations can be obtained by normalizing the gamma ray log (GRn) and porosity logs (neutron and density). Spectral gamma ray log (SGR) correlation for mineral classification for the Patala Formation is shown in Figure 6.

4.2.2. Porosity and Saturation. Porosity is the main component in estimating hydrocarbon saturation (%) and its existence. Density, neutron, and other logs commonly can be used to calculate porosity, whereas shale and its organic component affect the density.[48] Estimating total porosity in shale gas reservoirs poses a challenge due to high clay minerals and fine-grained texture.[49] Log porosity was used to generate a distribution map and to understand the regional porosity behavior. It can help understand the prospective of the Patala Formation compared to the surrounding fields having available logs. The geostatistical modeling of lateral porosity distribution in the Patala Formation reveals favorable porosity levels ranging from 10 to 44% in the study area, as shown in Figure 7. Notably, regions exhibit porosity levels ranging from 10 to 12%

https://doi.org/10.1021/acsomega.4c00465
ACS Omega 2024, 9, 15573−15589

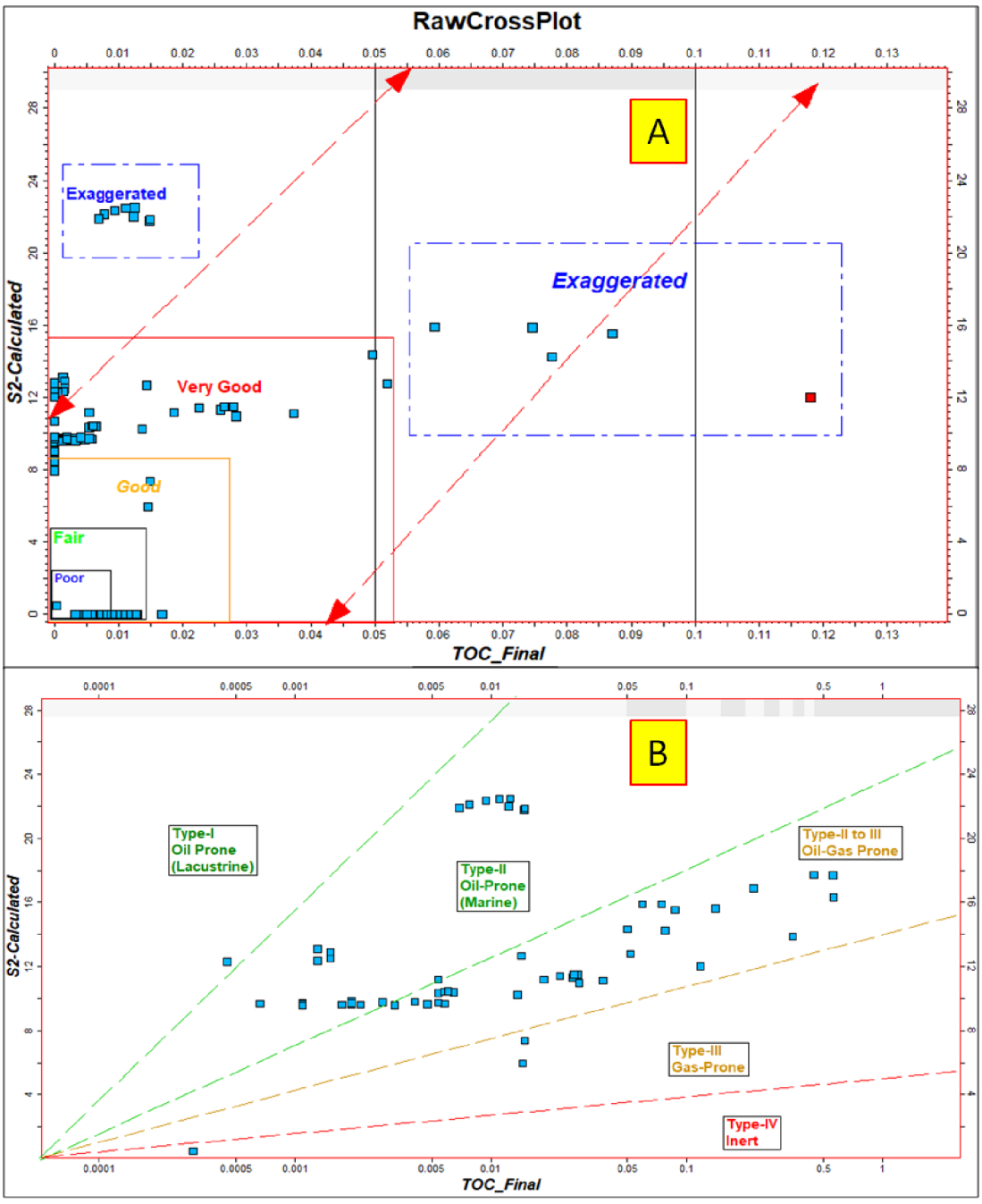

Figure 11. (A) Function for TOC vs S_2 for Patala Formation zone. (B) Kerogen types and qualitybased on a TOC-S_2 cross-plot.

and identified zones with porosity ranging from 40 to 44%. It may be due to the shallow depth of the formation experiencing less compaction, resulting in higher porosity.

After examining the relationship between the TOC and bulk density of formation and density data of some areas, Schmoker found an inversely proportional relationship (Figure 8). Regional well correlations for TOC estimation are shown in Figure 9. The linear relation between TOC and bulk density was established, and subsequently, it was found that shale rock density falls as the TOC value drops.[50]

Theoretically, the shale's organic matter density (1.02−1.11 g/cm^3) is less than that of the other part of the rock matrix. Therefore, because of the presence of organic matter in low porosity and permeability shale, rock formation density decreases as the organic content increases.[51]

4.3. Total Organic Carbon (TOC) Calculations. Accurate quantification and characterization of the TOC are crucial in exploring and developing hydrocarbon resources. To quantify TOC, various techniques have been employed, including laboratory-based geochemical analysis of source rock on core data and the utilization of well logs to develop mathematical correlations. These approaches aim to accurately estimate the TOC content and enhance our understanding of organic matter distribution in hydrocarbon reservoirs. In the case of unconventional and tight-rock systems, where extraction is more challenging, higher TOC values generally indicate larger volumes of hydrocarbons in place. By

https://doi.org/10.1021/acsomega.4c00465
ACS Omega 2024, 9, 15573−15589

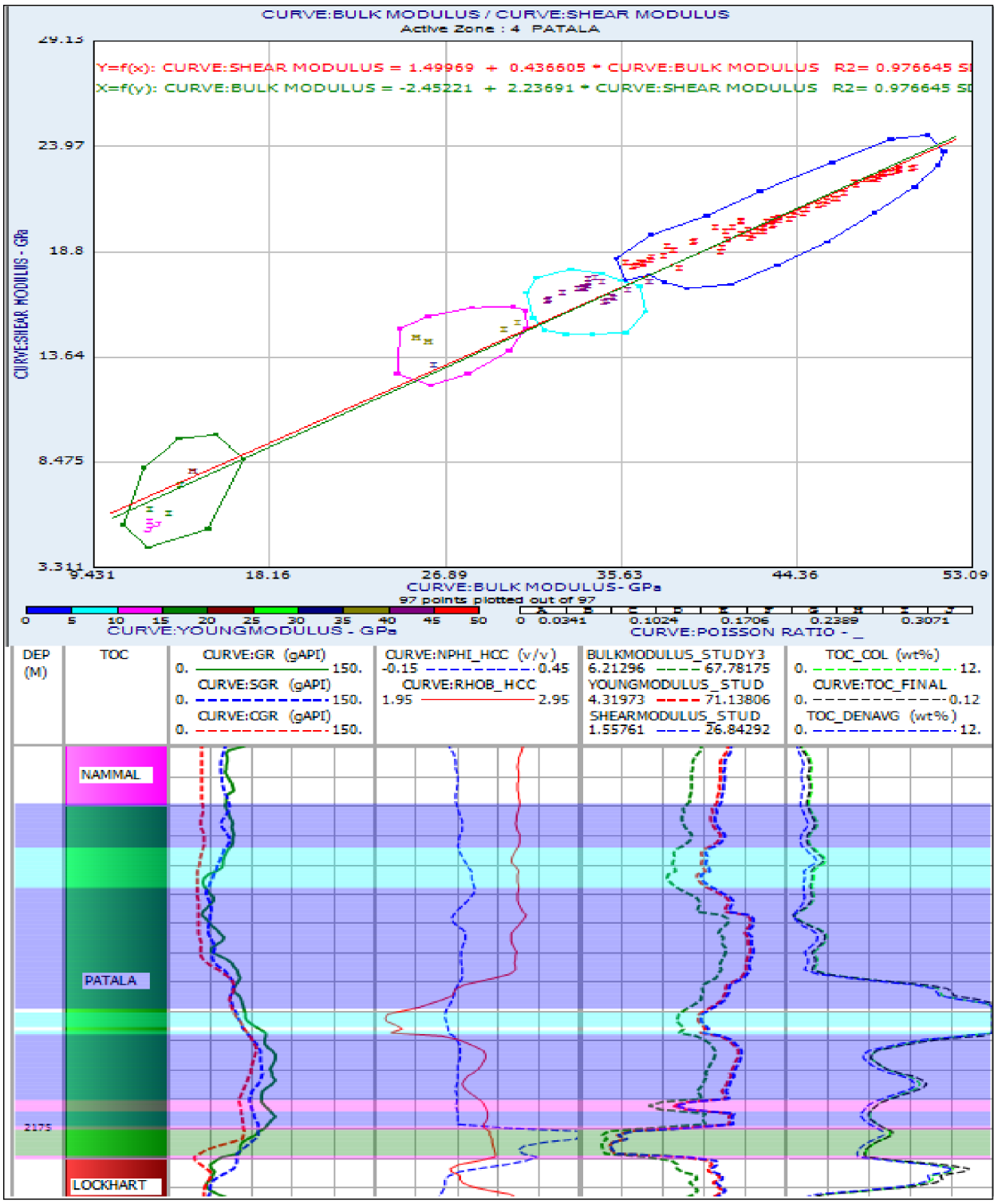

Figure 12. Bulk, shear, Young's moduli, Poisson's ratio relationship, and TOC estimation.

establishing a correlation between hydrocarbon storage and TOC, it becomes possible to comprehensively understand kerogen's connectivity and internal porosity, providing valuable insights for further exploration activities.[52,53]

The conditions within the depositional settings influence the quantity and composition of TOC present in the source rocks. The initiation of hydrocarbon generation typically occurs when organic matter is deposited in stagnant water conditions. Formations abundant in clay minerals, such as shale rocks, are often favorable for finding significant amounts of TOC. Generally, carbonate rocks may also contain relatively high levels of organic matter.[54] TOC calculation relies on many factors, such as gas adsorption, maturity, carbon content, and organic porosity. TOC is also affected by the pore texture and shale wettability. There are many methods to estimate TOC using well-log data, as petrophysical properties of the TOC are different in rock matrix parts.[55]

https://doi.org/10.1021/acsomega.4c00465
ACS Omega 2024, 9, 15573−15589

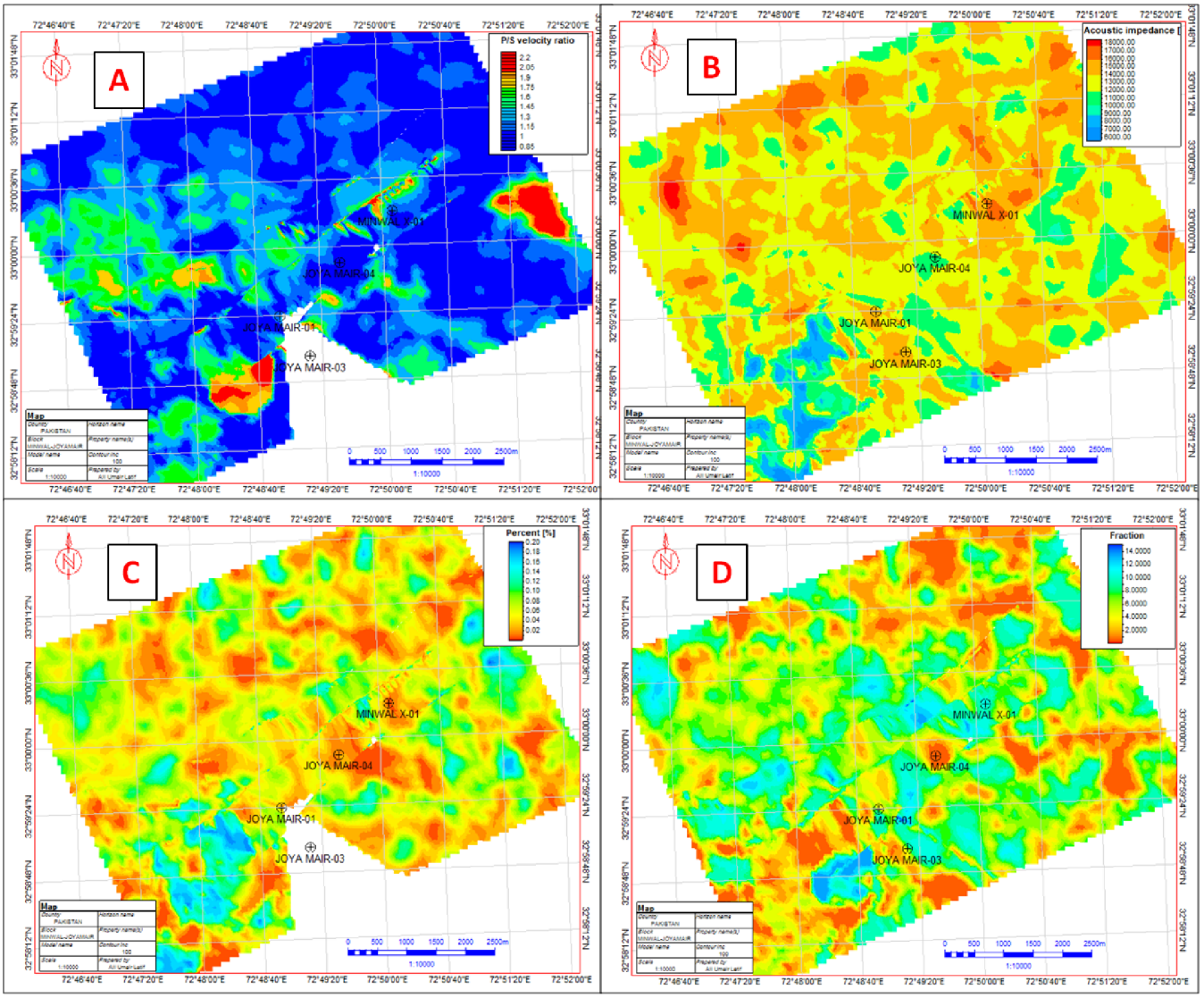

Figure 13. (A) $V_p/(V_s)$ ratio property map for the Patala Formation. (B) Patala Formation acoustic impedance property map. (C) TOC property map for the Patala Formation. (D) S_2 property map for the Patala Formation.

Table 2. Comparison of Different Methods for TOC Calculation

sample interval (m)	TOC value log calculated (wt %)	avg. log calculated (wt %)	literature value of TOC (wt %)	kerogen volume
2165	0.10	4.5	1.12−5.0	0.03
2166	0.00			0.03
2167	0.55			0.04
2168	0.33			0.03
2169	0.27			0.1
2170	0.43			0.12
2171	7.56			0.16
2172	18.48			0.37
2173	6.68			0.15
2174	6.02			0.14
2175	4.96			0.12
2176	5.54			0.1

Bulk density methodology was chosen to evaluate organic content. However, previous studies suggest that the improved and natural gamma spectroscopy methods are poor in accuracy.[56,57]

The neutron-density cross-plot shows specific variations of the Patala Formation as higher NPHI values and low RHOB values correspond to the net pay zone. It also depicts a more porous region as a preferable potential zone (Figure 10).

The cross-plot between TOC and S_2 shows that the Patala Formation lies mainly in the Type-II to Type-III zone and mostly has oil with minor gas. This also depicts the depositional environment of Formation, marine to the

https://doi.org/10.1021/acsomega.4c00465
ACS Omega 2024, 9, 15573−15589

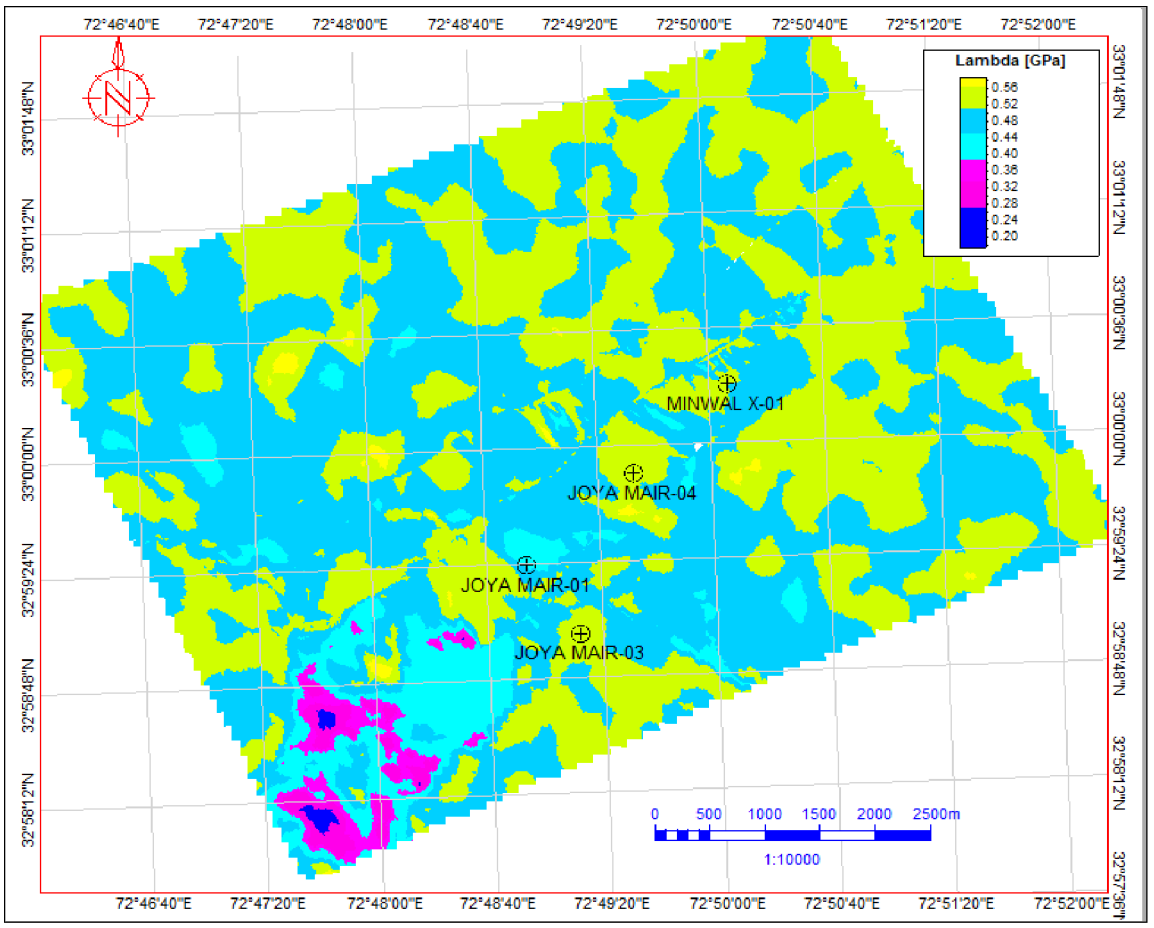

Figure 14. Brittleness index property map for the Patala Formation.

submarine environment (Figure 11a,b). The classification adopted from ref[58] is shown in Figure 11a,b).

The average calculated TOC value ranges from 4 to 6 wt %, with the TOC derived from sonic (TOC_DLRS) and Neutron (TOC_DLRN) log values less than 0.1 wt %, which can be due to the presence of disturbed borehole conditions (Table 2). Hence, the impact of the hole condition and logging errors were minimized by taking the average of all the calculated TOC values (TOC_DENAVG). The calculated TOC from the density logs is calibrated with available literature values for the Patala Formation, which is close to the estimate.

4.4. Elastic Moduli Relation with TOC Calculation. Elastic moduli are essential for unconventional shale reservoir characterization;[59] when integrated with other petrophysical properties, they become a valuable tool for reservoir characterization. Elastic moduli have some specific responsibilities related to the TOC value change.

Young's modulus and Poisson's ratio are considered crucial mechanical properties in the assessment of hydraulic fracture design, and these properties play a primary role in transforming vertical stress into horizontal stresses within the target Formation.[60] Previous studies conducted worldwide also indicate that as TOC content increases, Young's modulus and Poisson's ratio tend to decrease. Conversely, an increase in clay volume leads to a decrease in Young's modulus and an increase in Poisson's ratio.[61,62] Trends of decrease in Young's modulus with increasing TOC are expected since kerogen is a softer material than most other rock mineral constituents.[63] Poisson's ratio and Young's modulus cross-plot are used to determine the zone of brittleness in the Patala Formation. This cross-plot shows that the middle part of Formation (blue) is more ductile, which can be preferable for the future prospectively. It can also be depicted that a very small part of the Formation is brittle, making the Patala Formation prospective for unconventional exploration. In the current study, comparisons have also examined the relationship between TOC and Poisson's ratio, and Young's modulus, and these relationships are displayed in Figure 12.

Rock physics alone cannot be estimated for the highest TOC values but can give the best result combined with all of the petrophysical logs. Rock physics moduli are plotted along with the estimated TOC (Figure 12). The Patala Formation exhibits a strong correlation between Young's modulus and the TOC content, which depicts values decreasing as the TOC value increases. However, the TOC depends on elastic and petrophysical properties such as density, porosity, and saturation. These plots show different behavior as Spectrometry Gamma Ray (SGR) and CGR value changes affect the elastic moduli and ultimately affect the TOC values.

Previous studies suggest that the marine deposits found in the late Paleocene Patala Formation could serve as significant unconventional reservoirs for shale oil and gas in the Kohat-Potwar Plateau.[3] The Vp/(V s) ratio property map for the Patala Formation is displayed in Figure 13a, which shows 0.85−2.2 values. The acoustic impedance property map for the Patala Formation is displayed in Figure 13b, which shows 6000−18000 values. TOC and S_2 properties from well logs have been upscaled and populated in geomodel for regional

https://doi.org/10.1021/acsomega.4c00465
ACS Omega 2024, 9, 15573−15589

correlation along the Minwal-Joyamair Field (Figure 13c,d). The property map of TOC shows higher values around the Joyamair-04 and Minwal X-01 wells, as shown in Figure 13c. S_2 values need to be correlated with core data, which is not available for the current study, but log analysis of S_2 values shows higher prospective values around the Minwal X-01 well.

4.5. Brittleness Index. Shale geomechanical properties are essential for the effective design and application of hydraulic fracturing plans. Brittleness index (BI) is a crucial mechanical characteristic that plays a key role in assessing the fracturing potential of shale gas reservoirs, thereby influencing the selection of the appropriate hydraulic fracturing intervals. BI is a necessary tool for unconventional rock formation exploration. This method helps identify subsurface strata with a potentially high hydraulic fracturing susceptibility.[60,64−66]

The effective exploration of unconventional shale reservoirs by effective hydraulic fracturing is the basis for an economic and complete development. The most brittle rocks are essential for the successful hydraulic fracturing identification. For this reason, it is necessary to determine shale zone ductile and brittle zones. The BI has been calculated and estimated to identify the brittle and ductile zones based on brittleness indices. The predicted BI values ranged from 0.20 to 0.56 in the Patala Formation, as shown in Figure 14.

The brittleness index is upscaled along the model, and average maps are generated along each target horizon (formation). The BI property map shows this, which can be interpreted as most of the area being brittle in nature (Figure 14). These zones can be a potential zone of interest for future shale gas hydraulics stimulation for hydrocarbon production. Shale reservoirs that exhibit high porosity, high TOC, and high concentrations of brittle minerals are considered the "sweet spot" for optimal shale exploration.

5. CONCLUSIONS

The assessment procedure of shale gas reservoirs, which applied both well logs and seismic data, yielded a comprehensive comprehension of essential elastic and petrophysical characteristics. Research confirms that the Patala Formation is a proven source in this field. It can also be a potential for unconventional reservoir exploration. Petrophysical, rock physics, and geomechanical properties confirm that the Patala Formation can be a candidate for unconventional shale-gas exploration in the Potowar region. The petrophysical attributes extracted in this study of the Patala Formation characteristics provided the foundational groundwork for extensive shale resource exploration on the Kohat-Potwar Plateau. The organic matter, porosity, and brittleness index results make the Patala Formation an organic shale potential reservoir. In a nutshell, it has been concluded, based on an integrated study, that the Patala Formation possesses favorable factors (e.g., TOC content, thickness, and brittle mineral content) for a shale gas play that has the capacity to generate a significant volume of gas. It has been concluded that the Palaeocene Patala formation sediments demonstrate a high hydrocarbon potential.

AUTHOR INFORMATION

Corresponding Authors

Muhsan Ehsan − *School of Geosciences and Info-Physics, Central South University, Changsha 410083, China; Hunan Key Laboratory of Nonferrous Resources and Geological Hazards Exploration, Changsha 410083, China; Key Laboratory of Metallogenic Prediction of Nonferrous Metals, Ministry of Education, Central South University, Changsha 410083, China; Department of Earth and Environmental Sciences, Bahria School of Engineering and Applied Sciences, Bahria University, Islamabad 44000, Pakistan;* orcid.org/0000-0001-9430-5486; Email: muhsanehsan98@hotmail.com

Rujun Chen − *School of Geosciences and Info-Physics, Central South University, Changsha 410083, China; Hunan Key Laboratory of Nonferrous Resources and Geological Hazards Exploration, Changsha 410083, China; Key Laboratory of Metallogenic Prediction of Nonferrous Metals, Ministry of Education, Central South University, Changsha 410083, China*; Email: chrujun12358@gmail.com

Authors

Muhammad Ali Umair Latif − *Department of Earth and Environmental Sciences, Bahria School of Engineering and Applied Sciences, Bahria University, Islamabad 44000, Pakistan*

Kamal Abdelrahman − *Department of Geology and Geophysics, College of Science, King Saud University, Riyadh 11451, Saudi Arabia*

Abid Ali − *Institute of Geology, University of the Punjab, Lahore 54000, Pakistan*

Jar Ullah − *School of Geosciences and Info-Physics, Central South University, Changsha 410083, China;* orcid.org/0009-0003-1894-5010

Mohammed S. Fnais − *Department of Geology and Geophysics, College of Science, King Saud University, Riyadh 11451, Saudi Arabia*

Complete contact information is available at: https://pubs.acs.org/10.1021/acsomega.4c00465

Notes

The authors declare no competing financial interest.

ACKNOWLEDGMENTS

We thank the Directorate General Petroleum Concession (DGPC), Pakistan, for providing data for this research. We would like to thank Pakistan Oilfields Limited for their support and help in completing this work and software support. Furthermore, our special thanks and appreciation to LMK Resources Pakistan (Private) Limited (LMKR), Islamabad, Pakistan, GeoSoftware, Petrel software, and the Geophysical Lab of the Department of Earth and Environmental Sciences, Bahria University Islamabad, Pakistan, for providing the necessary platform and software to conduct this research within the stipulated time frame successfully. This research was funded by the Basic Science Centre Project of the National Natural Science Foundation of China, Grant Number 72088101. Special thanks and gratitude to the Researchers Supporting Project Number (RSP2024R351), King Saud University, Riyadh, Saudi Arabia, for funding this research article.

REFERENCES

(1) Khan, N.; Weltje, G. J.; Jan, I. U.; Swennen, R. Depositional and diagenetic constraints on the quality of shale-gas reservoirs: A case study from the Late Palaeocene of the Potwar Basin (Pakistan, Eastern Tethys). *Geol. J.* **2022**, *57* (7), 2770−2787.

(2) Xu, Z.; Li, X.; Li, J.; Xue, Y.; Jiang, S.; Liu, L.; Luo, Q.; Wu, K.; Zhang, N.; Feng, Y.; et al. Characteristics of Source Rocks and

https://doi.org/10.1021/acsomega.4c00465
ACS Omega 2024, 9, 15573−15589

Genetic Origins of Natural Gas in Deep Formations, Gudian Depression, Songliao Basin, NE China. *ACS Earth Space Chem.* **2022**, *6* (7), 1750−1771.
(3) Yasin, Q.; Baklouti, S.; Khalid, P.; Ali, S. H.; Boateng, C. D.; Du, Q. Evaluation of shale gas reservoirs in complex structural enclosures: A case study from Patala Formation in the Kohat-Potwar Plateau, Pakistan. *J. Pet. Sci. Eng.* **2021**, *198*, 108225.
(4) Javed, T.; Siyar, S. M.; Sajjad, S. M. W.; Ali, F.; Raziq, F.; Ullah, S.; Khan, N.; Ali, I. Hydrocarbon Source Rock Potential of the Late Paleocene Patala Formation, Kohat Basin, Pakistan; *Iran. J. Earth Sci.*, **2023**. .
(5) Yang, L.; Yang, D.; Zhang, M.; Meng, S.; Wang, S.; Su, Y.; Xu, L. Application of nano-scratch technology to identify continental shale mineral composition and distribution length of bedding interfacial transition zone - A case study of Cretaceous Qingshankou formation in Gulong Depression, Songliao Basin, NE China. *Geoenergy Sci. Eng.* **2024**, *234*, 212674.
(6) Sohail, G. M.; Hawkes, C. D.; Yasin, Q. An integrated petrophysical and geomechanical characterization of Sembar Shale in the Lower Indus Basin, Pakistan, using well logs and seismic data. *J. Nat. Gas Sci. Eng.* **2020**, *78*, 103327.
(7) Aziz, H.; Ehsan, M.; Ali, A.; Khan, H. K.; Khan, A. Hydrocarbon source rock evaluation and quantification of organic richness from correlation of well logs and geochemical data: A case study from the sembar formation, Southern Indus Basin, Pakistan. *J. Nat. Gas Sci. Eng.* **2020**, *81*, 103433.
(8) Xi, Z.; Xiaoming, Z.; Jiawang, G.; Shuxin, L.; Tingshan, Z.. *Karst topography paces the deposition of lower Permian, organic-rich, marine−continental transitional shales in the southeastern Ordos Basin, northwestern China*; AAPG Bulletin, 2023. .
(9) Khalil Khan, H.; Ehsan, M.; Ali, A.; Amer, M. A.; Aziz, H.; Khan, A.; Bashir, Y.; Abu-Alam, T.; Abioui, M. Source rock geochemical assessment and estimation of TOC using well logs and geochemical data of Talhar Shale, Southern Indus Basin, Pakistan. *Front. Earth Sci.* **2022**, *10*, 969936.
(10) Ashraf, U.; Zhang, H.; Anees, A.; Ali, M.; Zhang, X.; Shakeel Abbasi, S.; Nasir Mangi, H. Controls on Reservoir Heterogeneity of a Shallow-Marine Reservoir in Sawan Gas Field, SE Pakistan: Implications for Reservoir Quality Prediction Using Acoustic Impedance Inversion. *Water* **2020**, *12* (11), 2972.
(11) Li, Q.; Lu, L.; Zhao, Q.; Hu, S. Impact of Inorganic Solutes' Release in Groundwater during Oil Shale In Situ Exploitation. *Water* **2023**, *15* (1), 172.
(12) Yang, L.; Wang, H.; Xu, H.; Guo, D.; Li, M. Experimental study on characteristics of water imbibition and ion diffusion in shale reservoirs. *Geoenergy Sci. Eng.* **2023**, *229*, 212167.
(13) Ullah, J.; Luo, M.; Ashraf, U.; Pan, H.; Anees, A.; Li, D.; Ali, M.; Ali, J. Evaluation of the geothermal parameters to decipher the thermal structure of the upper crust of the Longmenshan fault zone derived from borehole data. *Geothermics* **2022**, *98*, 102268.
(14) Xu, G.; Haq, B. U. Seismic facies analysis: Past, present and future. *Earth-Sci. Rev.* **2022**, *224*, 103876.
(15) Khalid, P.; Farid, A.; Naseer, M. T.; Yasin, Q.; Naseem, S. Seismic stratigraphy and attributes application for imaging a Lower Cretaceous deltaic system: Sukkur rift zone, Lower Indus Basin, Pakistan. *Mar. Pet. Geol.* **2022**, *149*, 106030.
(16) Wang, Y.; Peng, J.; Wang, L.; Xu, C.; Dai, B. Micro-macro evolution of mechanical behaviors of thermally damaged rock: A state-of-the-art review; *J. Rock Mech. Geotech. Eng.*, 2023. .
(17) Xu, Y.; Lun, Z.; Pan, Z.; Wang, H.; Zhou, X.; Zhao, C.; Zhang, D. Occurrence space and state of shale oil: A review. *J. Pet. Sci. Eng.* **2022**, *211*, 110183.
(18) Li, J.; Zhang, Y.; Lin, L.; Zhou, Y. Study on the shear mechanics of gas hydrate-bearing sand-well interface with different roughness and dissociation. *Bull. Eng. Geol. Environ.* **2023**, *82* (11), 404.
(19) Kumar, S.; Ojha, K.; Bastia, R.; Garg, K.; Das, S.; Mohanty, D. Evaluation of Eocene source rock for potential shale oil and gas generation in north Cambay Basin, India. *Mar. Pet. Geol.* **2017**, *88*, 141−154.
(20) Cavelan, A.; Boussafir, M.; Rozenbaum, O.; Laggoun-Défarge, F. Organic petrography and pore structure characterization of low-mature and gas-mature marine organic-rich mudstones: Insights into porosity controls in gas shale systems. *Mar. Pet. Geol.* **2019**, *103*, 331−350.
(21) Zhou, J.; Tian, S.; Xian, X.; Zheng, Y.; Yang, K.; Liu, J. Comprehensive review of property alterations induced by CO_2−shale interaction: implications for CO_2 sequestration in shale. *Energy Fuels* **2022**, *36* (15), 8066−8080.
(22) Mandal, P. P.; Sarout, J.; Rezaee, R. Triaxial Deformation of the Goldwyer Gas Shale at In Situ Stress Conditions—Part I: Anisotropy of Elastic and Mechanical Properties. *Rock Mech. Rock Eng.* **2022**, *55* (10), 6121−6149.
(23) Wang, Y.; Wang, Z.; Zhang, Z.; Yao, S.; Zhang, H.; Zheng, G.; Luo, F.; Feng, L.; Liu, K.; Jiang, L. Recent techniques on analyses and characterizations of shale gas and oil reservoir. *Energy Reviews* **2024**, *3*, 100067.
(24) Swati, M. A. F.; Hanif, M.; Haneef, M.; Saboor, A. Late Palaeocene to Early Eocene biostratigraphic framework from Upper Indus Basin, Pakistan, Eastern Tethys. *Geol. J.* **2021**, *56* (7), 3541−3556.
(25) Latif, M. A. U.; Ehsan, M.; Ali, M.; Ali, A.; Ekoa Bessa, A. Z.; Abioui, M. The assessment of reservoir potential of Permian to Eocene reservoirs of Minwal-Joyamair fields, upper Indus basin, Pakistan. *Heliyon* **2023**, *9* (6), No. e16517.
(26) Amjad, M. R.; Ehsan, M.; Hussain, M.; Al-Ansari, N.; Rehman, A.; Naseer, Z.; Ejaz, M. N.; Baouche, R.; Elbeltagi, A. Carbonate Reservoir Quality Variations in Basins with a Variable Sediment Influx: A Case Study from the Balkassar Oil Field, Potwar, Pakistan. *ACS Omega* **2023**, *8* (4), 4127−4145.
(27) Ehsan, M.; Latif, M. A. U.; Ali, A.; Radwan, A. E.; Amer, M. A.; Abdelrahman, K. Geocellular Modeling of the Cambrian to Eocene Multi-Reservoirs, Upper Indus Basin, Pakistan. *Nat. Resour. Res.* **2023**, *32* (6), 2583−2607.
(28) Kazmi, A. H.; Jan, M. Q.. *Geology and Tectonics of Pakistan*; Graphic publishers: Karachi, Pakistan, 1997; pp 528.
(29) Jaswal, T. M.; Lillie, R. J.; Lawrence, R. D. Structure and evolution of the northern Potwar deformed zone, Pakistan. *AAPG Bull.* **1997**, *81* (2), 308−328.
(30) Fazeelat, T.; Jalees, M.; Bianchi, T. Source rock potential of Eocene, Paleocene and Jurassic deposits in the subsurface of the Potwar Basin, northern Pakistan. *J. Pet. Geol.* **2010**, *33* (1), 87−96.
(31) Wandrey, C. J.; Law, B.; Shah, H. A.. *Patala-Nammal composite total petroleum system, Kohat-Potwar geologic province, Pakistan*; US Department of the Interior, US Geological Survey, 2004.
(32) Khan, N.; Anjum, N.; Ahmad, M.; Awais, M.; Ullah, N. Hydrocarbon source rock potential evaluation of the Late Paleocene Patala Formation, Salt Range, Pakistan: Organic geochemical and palynofacies approach. *J. Earth Syst. Sci.* **2018**, *127* (7), 98.
(33) Shah, S. I.. *Stratigraphy of Pakistan. Geological Survey of Pakistan*; Government of Pakistan Ministry of Petroleum & Natural Resorces: Islamabad, Pakistan, 2009; Vol. *22*, pp 381.
(34) Kadri, I. B.. *Petroleum geology of Pakistan*; Pakistan Petroleum Limited Karachi: Pakistan, 1995; pp 375.
(35) Ahmad, S.; Ahmad, F.; Ullah, A.; Eisa, M.; Ullah, F.; Kaif, K.; Khan, S. Integration of the outcrop and subsurface geochemical data: implications for the hydrocarbon source rock evaluation in the Lower Indus Basin, Pakistan. *J. Pet. Explor. Prod. Technol.* **2019**, *9* (2), 937−951.
(36) Yu, H.; Rezaee, R.; Wang, Z.; Han, T.; Zhang, Y.; Arif, M.; Johnson, L. A new method for TOC estimation in tight shale gas reservoirs. *Int. J. Coal Geol.* **2017**, *179*, 269−277.
(37) Schmoker, J. W. Determination of Organic Content of Appalachian Devonian Shales from Formation-Density Logs: GEOLOGIC NOTES. *AAPG Bull.* **1979**, *63* (9), 1504−1509.
(38) Passey, Q.; Creaney, S.; Kulla, J.; Moretti, F.; Stroud, J. A practical model for organic richness from porosity and resistivity logs. *AAPG Bull.* **1990**, *74* (12), 1777−1794.

https://doi.org/10.1021/acsomega.4c00465
ACS Omega 2024, 9, 15573−15589

(39) Schmoker, J. W.; Hester, T. C. Organic carbon in Bakken formation, United States portion of Williston basin. *AAPG Bull.* **1983**, *67* (12), 2165−2174.
(40) Wang, H.; Wu, W.; Chen, T.; Dong, X.; Wang, G. An improved neural network for TOC, S1 and S2 estimation based on conventional well logs. *J. Pet. Sci. Eng.* **2019**, *176*, 664−678.
(41) Mavko, G.; Mukerji, T.; Dvorkin, J.. *The rock physics handbook*; Cambridge university press, 2020.
(42) Xu, H.; Zhou, W.; Hu, Q.; Yi, T.; Ke, J.; Zhao, A.; Lei, Z.; Yu, Y. Quartz types, silica sources and their implications for porosity evolution and rock mechanics in the Paleozoic Longmaxi Formation shale, Sichuan Basin. *Mar. Pet. Geol.* **2021**, *128*, 105036.
(43) Xie, W.; Chen, S.; Gan, H.; Wang, H.; Wang, M.; Vandeginste, V. Preservation conditions and potential evaluation of the Longmaxi shale gas reservoir in the Changning area, southern Sichuan Basin. *Geosci. Lett.* **2023**, *10* (1), 36.
(44) Sohail, G. M.; Radwan, A. E.; Mahmoud, M. A review of Pakistani shales for shale gas exploration and comparison to North American shale plays. *Energy Rep.* **2022**, *8*, 6423−6442.
(45) de Jonge-Anderson, I.; Ma, J.; Wu, X.; Stow, D. Determining reservoir intervals in the Bowland Shale using petrophysics and rock physics models. *Geophys. J. Int.* **2021**, *228* (1), 39−65.
(46) Ardebili, P. N.; Jozanikohan, G.; Moradzadeh, A. Estimation of porosity and volume of shale using artificial intelligence, case study of Kashafrud Gas Reservoir, NE Iran. *J. Pet. Explor. Prod. Technol.* **2024**, *14*, 477−494.
(47) Huang, R.; Wang, Y.; Cheng, S.; Liu, S.; Cheng, L. Selection of logging-based TOC calculation methods for shale reservoirs: A case study of the Jiaoshiba shale gas field in the Sichuan Basin. *Nat. Gas Ind. B* **2015**, *2* (2−3), 155−161.
(48) Jadoon, Q. K.; Roberts, E.; Blenkinsop, T.; Raphael, A.; Shah, S. A. Mineralogical modelling and petrophysical parameters in Permian gas shales from the Roseneath and Murteree formations, Cooper Basin, Australia. *Pet. Explor. Dev.* **2016**, *43* (2), 277−284.
(49) Tang, Q.; Gratchev, I. Estimation of sedimentary rock porosity using a digital image analysis. *Appl. Sci.* **2023**, *13* (4), 2066.
(50) Jiang, S.; Mokhtari, M.; Borrok, D.; Lee, J. Improving the total organic carbon estimation of the Eagle Ford shale with density logs by considering the effect of pyrite. *Minerals* **2018**, *8* (4), 154.
(51) Schwartz, B.; Huffman, K.; Thornton, D.; Elsworth, D. The effects of mineral distribution, pore geometry, and pore density on permeability evolution in gas shales. *Fuel* **2019**, *257*, 116005.
(52) Sun, C.; Nie, H.; Dang, W.; Chen, Q.; Zhang, G.; Li, W.; Lu, Z. Shale gas exploration and development in China: Current status, geological challenges, and future directions. *Energy Fuels* **2021**, *35* (8), 6359−6379.
(53) Muther, T.; Qureshi, H. A.; Syed, F. I.; Aziz, H.; Siyal, A.; Dahaghi, A. K.; Negahban, S. Unconventional hydrocarbon resources: geological statistics, petrophysical characterization, and field development strategies. *J. Pet. Explor. Prod. Technol.* **2022**, *12* (6), 1463−1488.
(54) McCarthy, K.; Rojas, K.; Niemann, M.; Palmowski, D.; Peters, K.; Stankiewicz, A. Basic petroleum geochemistry for source rock evaluation. *Oilfield Rev.* **2011**, *23* (2), 32−43.
(55) Asif, M.; Fazeelat, T.; Jalees, M. I. Biomarker and stable carbon isotopic study of Eocene sediments of North-Western Potwar Basin, Pakistan. *J. Pet. Sci. Eng.* **2014**, *122*, 729−740.
(56) Mahmoud, A. A.; Elkatatny, S.; Ali, A. Z.; Abouelresh, M.; Abdulraheem, A. Evaluation of the Total Organic Carbon (TOC) Using Different Artificial Intelligence Techniques. *Sustainability* **2019**, *11* (20), 5643.
(57) Yan, T.; Xu, R.; Sun, S.-H.; Hou, Z.-K.; Feng, J.-Y. A real-time intelligent lithology identification method based on a dynamic felling strategy weighted random forest algorithm; *Petroleum Science*, 2023 .
(58) Peter, K. E.; Cassa, M. R. Applied Source Rock Geochemistry. In *The petroleum system from source to trap*; AAPG MEMOIR, 1994; vol. *60*, pp 95.
(59) Yao, W.; Yu, J.; Liu, X.; Zhang, Z.; Feng, X.; Cai, Y. Experimental and theoretical investigation of coupled damage of rock under combined disturbance. *Int. J. Rock Mech. Min. Sci.* **2023**, *164*, 105355.
(60) Yasin, Q.; Du, Q.; Sohail, G. M.; Ismail, A. Fracturing index-based brittleness prediction from geophysical logging data: application to Longmaxi shale. *Geomech. Geophys. Geo-Energy. Georesour.* **2018**, *4*, 301−325.
(61) Mode, A. W.; Willie, E. S.; Eradiri, J. N.; Umeadi, M. I. Geochemical and mineralogical controls on the geomechanical properties of the Eze-Aku Shale: Implications for a potential hydrocarbon reservoir. *J. Afr. Earth Sci.* **2022**, *196*, 104698.
(62) Omovie, S. J.; Castagna, J. P. Relationships between dynamic elastic moduli in shale reservoirs. *Energies* **2020**, *13* (22), 6001.
(63) Alafnan, S. Utilization of supercritical carbon dioxide for mechanical degradation of organic matters contained in shales. *Fuel* **2022**, *316*, 123427.
(64) Ren, C.; Yu, J.; Liu, S.; Yao, W.; Zhu, Y.; Liu, X. A Plastic Strain-Induced Damage Model of Porous Rock Suitable for Different Stress Paths. *Rock Mech. Rock Eng.* **2022**, *55* (4), 1887−1906.
(65) Ye, Y.; Tang, S.; Xi, Z.; Jiang, D.; Duan, Y. A new method to predict brittleness index for shale gas reservoirs: Insights from well logging data. *J. Pet. Sci. Eng.* **2022**, *208*, 109431.
(66) Lei, W.; Liu, X.; Ding, Y.; Xiong, J.; Liang, L. The investigation on shale mechanical characteristics and brittleness evaluation. *Sci. Rep.* **2023**, *13* (1), 22936.

https://doi.org/10.1021/acsomega.4c00465
ACS Omega 2024, 9, 15573−15589